Environ. Sci. Technol. **2006**, *40*, 370−376

Environmentally Benign Hardness Removal Using Ion-Exchange Fibers and Snowmelt

JOHN E. GREENLEAF AND ARUP K. SENGUPTA*

Department of Civil and Environmental Engineering, Lehigh University, 13 East Packer Avenue, Bethlehem, Pennsylvania 18015

Many industrial unit operations and unit processes require near-complete removal of hardness to avoid scaling in heat-transfer equipment, fouling in membranes, and high consumption of detergents and sequestering chemicals in cooling and wash water. Lime softening and cation exchange are the most commonly used processes practiced to date for hardness removal. Herein, we report and discuss the results and attributes of a new hardness removal process using ion-exchange fibers (IX-fibers). Most importantly, the process uses harvested snowmelt (or rainwater) as the regenerant chemical along with sparged carbon dioxide. Consequently, the spent regenerant does not contain a high concentration of aggressive chemicals such as sodium chloride or acid like traditional ion-exchange processes nor does the process produce voluminous sludges similar to lime softening. The bulk of carbon dioxide consumed during regeneration remains sequestered in the aqueous phase as alkalinity. IX-fibers form the heart of the process. They are essentially thin cylindrical polymeric strands 10−20 μm in diameter. The weak-acid carboxylate functional groups reside near to the surface of these cylindrical fibers. Low intraparticle diffusional resistance is the underlying reason IX-fibers are amenable to efficient regeneration with snowmelt sparged with carbon dioxide. When the carbon dioxide partial pressure is increased to 6.8 atm, over 90% calcium desorption efficiency is obtained. On the contrary, commercial weak-acid ion-exchange resins in spherical bead forms are ineffective for regeneration with carbon-dioxide-sparged snowmelt due to extremely slow ion-exchange kinetics involving counter-transport of Ca^{2+} and H^+.

Introduction

Removal of hardness from water is a treatment or pretreatment practiced in a wide variety of installations including chemical industries, power plants, laundries, individual households, and drinking water treatment plants, to name a few. With the recent growth in pressure-driven membrane processes (e.g., reverse osmosis and nanofiltration), removal of hardness through pretreatment has attained special significance in protecting the health and durability of membranes. Low- and medium-pressure steam generators often require large volumes of hardness-free water as the feed. The two universally practiced processes for hardness removal are lime softening and ion exchange. While lime softening produces voluminous sludge to be disposed, ion-exchange processes generate concentrated brine or mineral acid as a waste regenerant stream (*1*−*4*). Residuals management will continue to be a major concern with these processes. One major shortcoming of an ion-exchange-type separation process is the use of concentrated aggressive chemicals such as acid, salt, or alkali as regenerants and consequent difficulties in disposing of these waste regenerant streams.

The subject paper discusses the possible use of thin cylindrical ion-exchange fibers (IX-fibers) in place of traditional spherical resin beads for removal of hardness. In IX-fibers, the functional groups reside predominantly on the surface. During the past decade, the preparation and production of IX-fibers have come of age and several potential applications have been reported (*5*−*12*). The proposed softening process takes advantage of the unique physical configuration of the IX-fibers in a way that carbon-dioxide-sparged rainwater or snowmelt can be used as the sole regenerant, thus generating no aggressive waste. The complete absence of alkalinity in harvested rainwater or snowmelt makes them ideally suited as a regenerant. Carbon dioxide has previously been used as a regenerant for mixed-bed ion-exchange resins to partially desalinate water (*13*, *14*). However, the use of harvested rainwater/snowmelt along with ion-exchange fibers embodies the attributes of an environmentally benign process for hardness removal not investigated to date.

Process Chemistry and Underlying Chemistry

Ion-exchange fibers containing carboxylate (−COOH) functional groups form the heart of the process. The fibers are essentially hard long cylinders with diameters less than 20 μm. Like spherical ion-exchange resin beads, the fibers can be used in a fixed-bed column, and the following constitute the two primary steps of the process:

Step 1. Hardness Removal by the Ion-Exchange Fibers.

$$2\overline{\text{F}-\text{COOH}} + \text{Ca}(\text{HCO}_3)_2 \leftrightarrow \overline{(\text{F}-\text{COO})_2\text{Ca}} + 2\text{H}_2\text{CO}_3 \quad (1)$$

$$2\overline{\text{F}-\text{COOH}} + \text{Mg}(\text{HCO}_3)_2 \leftrightarrow \overline{(\text{F}-\text{COO})_2\text{Mg}} + 2\text{H}_2\text{CO}_3 \quad (2)$$

F represents the fiber matrix, and the overbar denotes the solid phase. Sodium ion is also removed, but its affinity is significantly lower than that of the divalent ions.

Step 2. Regeneration with Carbon-Dioxide-Sparged Rainwater/Snowmelt. Three important steps of carbon dioxide regeneration are

$$2\text{CO}_2(\text{g}) + 2\text{H}_2\text{O} \leftrightarrow 2\text{H}_2\text{CO}_3(\text{aq}) \quad \text{p}K_\text{H} = 1.41 \text{ at } 20\ ^\circ\text{C} \quad (3)$$

$$2\text{H}_2\text{CO}_3(\text{aq}) \leftrightarrow 2\text{H}^+ + 2\text{HCO}_3^- \quad \text{p}K_{\text{a1}} = 6.38 \text{ at } 20\ ^\circ\text{C} \quad (4)$$

$$\overline{(\text{F}-\text{COO})_2\text{Ca}} + 2\text{H}^+ \leftrightarrow 2\overline{\text{F}-\text{COOH}} + \text{Ca}^{2+} \quad (5)$$

Overall

$$\overline{(\text{F}-\text{COO})_2\text{Ca}} + 2\text{CO}_2(\text{g}) + 2\text{H}_2\text{O} \leftrightarrow 2\overline{(\text{F}-\text{COOH})} + \text{Ca}^{2+} + 2\text{HCO}_3^- \quad (6)$$

* Corresponding author phone: (610)758-3534; fax: (610)758-6405; e-mail: arup.sengupta@lehigh.edu.

10.1021/es051702x CCC: $33.50 © 2006 American Chemical Society
Published on Web 11/19/2005

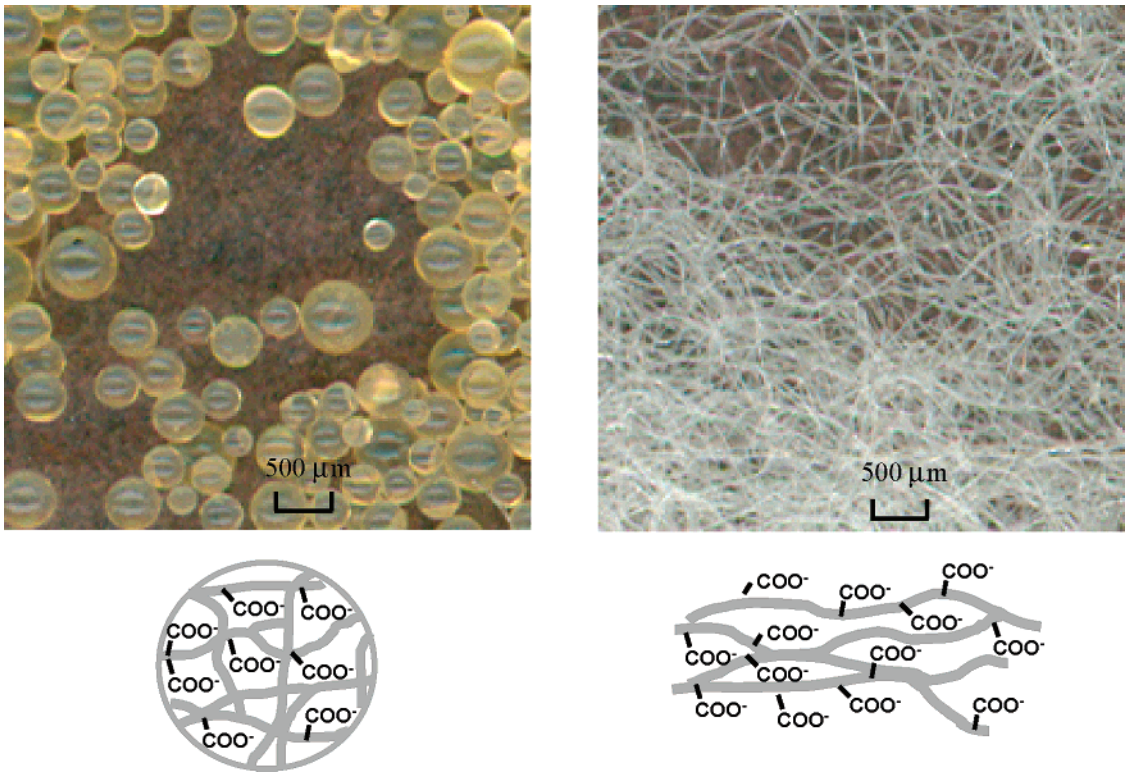

FIGURE 1. Weak-acid ion-exchange resin beads and fibers at 10× magnification with schematic illustrations.

TABLE 1. Salient Properties of Weak-Acid Cation Resin (C-104) and Ion-Exchange Fibers (Fiban K-4)

	C-104 resin	Fiban K-4 fiber
diameter	500−1200 μm	10−50 μm
capacity (dry)	9−10 mequiv/g	4−5 mequiv/g
shape	R−COO^-	F−COO^- identical
configuration	fixed bed	fixed bed

From a mass balance perspective, no additional chemicals/salts are present in the regenerant waste. From an equilibrium viewpoint, the above-mentioned reactions (eqs 1−5) are equally applicable for commercial weak-acid cation-exchange resins. However, the mechanism of sorption/desorption kinetics, as explained later in the paper, is intrinsically different between IX-fibers and commercial resin beads. Specific objectives of the investigation are to:

- demonstrate through convincing experimental evidence that IX-fibers can remove hardness and be regenerated efficiently with CO_2-sparged snowmelt;
- confirm the poor desorption efficiency of commercial ion-exchange resins under identical conditions;
- elucidate the effects of the carbon dioxide partial pressure and the sorption/desorption mechanism for commercial resin beads and fibers.

Materials and Methods

Ion-Exchange Resin and Fiber. The resin used is a standard, spherical, microporous (gel) polyacrylic resin cross-linked with divnylbenzene (Purolite C-104, Purolite Co., Philadelphia, PA). The fibers are composed of loosely packed strands and available from UP Unitechprom BSU, Belarus. Both materials have carboxylate functional groups, and Figure 1 shows photographs of the cylindrical fibers and resin beads. Prior to laboratory use, resin and fibers were pretreated with 1 N HCl for 1 h, thoroughly rinsed with distilled water, and then air-dried. Table 1 provides the pertinent information about the fibers and resins used in the study.

Fixed-Bed Column Runs and Carbon Dioxide Regeneration. Fixed-bed column runs were carried out using epoxy-coated glass columns (11 mm in diameter), constant-flow stainless steel pumps, and an ISCO fraction collector. The ratio of column diameter to exchanger bead or fiber diameter was approximately 20:1; earlier work on chromate, pentachlorophenol, and phosphate removals with similar setups showed no premature leakage due to wall effects under identical conditions (*15*−*17*). The superficial liquid velocity (SLV) and the empty bed contact time (EBCT) were recorded for each column run. All calcium was in the form of temporary hardness. Figure 2 provides the schematic of the CO_2-sparged regeneration system for both IX-fibers and resins.

Snowmelt resulting from snows collected during February 2003 at the Lehigh University campus was used as the primary regenerant solution. The pressurized regenerant solution chamber could be sparged with carbon dioxide (Airgas Corporation, PA) at varying pressures up to 100 psig. A stainless steel pump and a throttling valve were used to control the flow rate of the regenerant solution while an ISCO fraction collector collected samples at predetermined time intervals. The snowmelt had a conductivity of 19 μs/cm, and the concentrations of chloride, nitrate, and sulfate in the snowmelt were 0.4, 2.3, and 2.1 mg/L, respectively.

Shrinking Tests with Light Microscopy. Light microscopy was used to evaluate shrinking tests for fiber and resin samples. Light microscopy was performed on a Westover Scientific Micromaster I binocular light microscope. Objective lenses of 10× and 40× magnifications were used for resin and fibrous materials, respectively. Fiber and resin samples in calcium forms were placed on a glass slide and covered with a cover slip. A small amount of water was added at the edges. To observe the effects of swelling and shrinkage, a few drops of 0.25 M HCl were added at the edges of the cover slip. All pictures of particles and measurements of particle diameters were made using a magnetic circular dichroism (MCD) digital microscope head attached to the light microscope head and a laptop computer. Digital camera measurements were calibrated using calibration slides prior

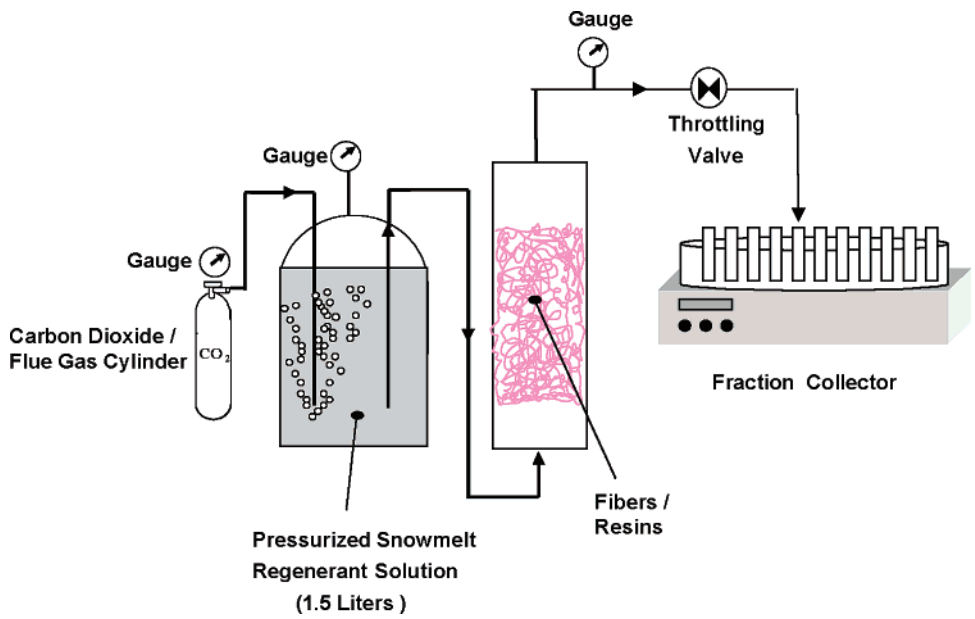

FIGURE 2. Laboratory setup depicting the CO_2-sparged snowmelt system used in the regeneration of both fiber and resin ion-exchange materials.

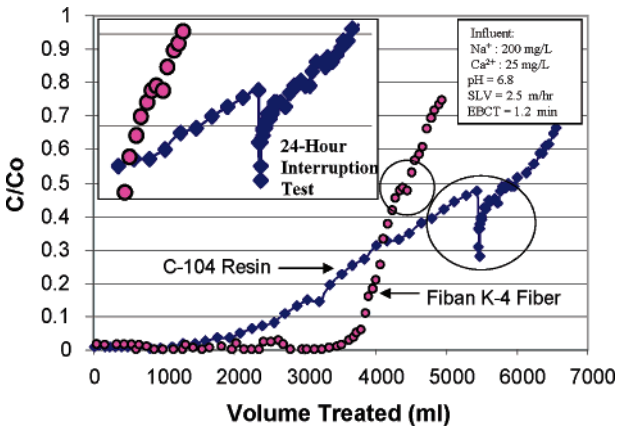

FIGURE 3. Fixed-bed column runs for hardness removal using two different ion-exchange materials under otherwise identical conditions: EBCT = empty bed contact time; SLV = superficial liquid velocity.

to data acquisition. All calibrations and measurements were made in the units of micrometers.

Results

Column Runs: Spherical Resin Beads versus Ion-Exchange Fibers. Figure 3 shows a comparison of two fixed-bed column runs under identical conditions; one run used the weak-acid cation-exchange resin (C-104, Purolite Co.), while the other used Fiban K-4 weak-acid IX-fiber. The influent composition and hydrodynamic conditions (i.e., EBCT and SLV) were the same and provided in Figure 3. The chemical composition of the functional group and the hardness removal mechanism were identical in both cases. Although the overall calcium removal capacity was significantly greater for the spherical resin beads, the calcium breakthrough from the IX-fiber column was much sharper. The 10% of influent calcium breakthrough occurred at less than 3000 mL of solution throughput for C-104 resin. In comparison, with the IX-fiber column, the same breakthrough occurred at nearly 4000 mL. Previous studies also demonstrated sharper breakthroughs and faster sorption kinetics with IX-fibers for selective separation of other ions of interest (*6*, *18*−*21*).

During each of the two column runs, as the calcium gradually started exiting the column, the influent flow was deliberately discontinued for 24 h. When the flow was subsequently resumed, the calcium concentration at the exit of each column was analyzed for any possible changes. An enlarged view of the interruption test is provided in the inset of Figure 3. Note that there was only very little change in the calcium concentration exiting from the fiber column. For the weak-acid resin, however, a significant drop in the calcium concentration was readily observed. After the restart and the subsequent passage of several hundred bed volumes of the influent solution, calcium eventually reached the concentration prior to interruption.

Successive Runs. Three successive column runs with IX-fibers were carried out at different calcium feed concentrations but under identical hydrodynamic conditions. Between runs, the fibers were regenerated with carbon-dioxide-sparged snowmelt at 5 atm. Figure 4A shows normalized calcium effluent histories where C_0 and C are the calcium concentrations in the influent and in the exit at any time, respectively. The abscissa (x-axis) of the effluent history plot was normalized with respect to equivalents of calcium ions fed to the columns for each run. The competing sodium ion concentration for every run was 200 mg/L as Na. Figure 4B is a bar chart showing calcium removal capacities for the three runs. Note that the calcium removal capacity is nearly identical for all three runs with different calcium concentrations in the feed.

Regeneration. Snowmelt collected from the precipitation at the Lehigh University campus during the month of February in 2003 was used for regeneration. Figures 5A and 5B show concentration profiles of calcium during regeneration of calcium-loaded IX-fibers and resin beads at different carbon dioxide partial pressures, all other conditions remaining identical. Note that calcium desorption for C-104 is noticeably poor in comparison with IX-fibers. Figure 6 provides bar charts showing percentage recoveries of calcium for both IX-fibers and weak-acid resins at different carbon dioxide partial pressures. An increase in partial pressure of carbon dioxide always resulted in higher calcium recovery.

Batch Desorption and Ca^{2+}/H^+ Relative Affinity. Relative affinity of calcium (Ca^{2+}) and hydrogen ion (H^+) toward IX-fibers with carboxylate functional groups and their exchange kinetics are centrally responsible for the success of the

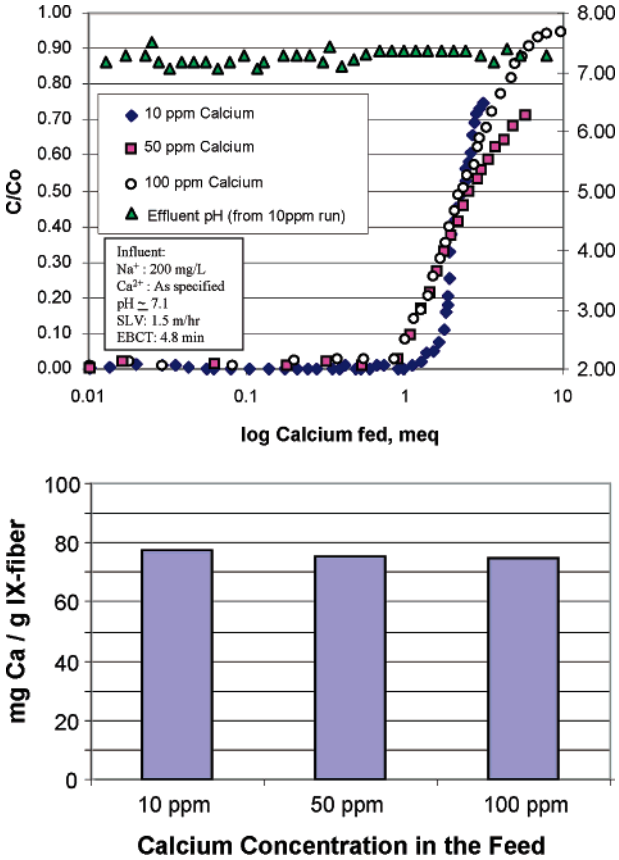

FIGURE 4. (a) Successive column runs at varying calcium feed concentrations using IX-fibers. (b) Calcium removal capacity of the IX-fiber for each feed concentration.

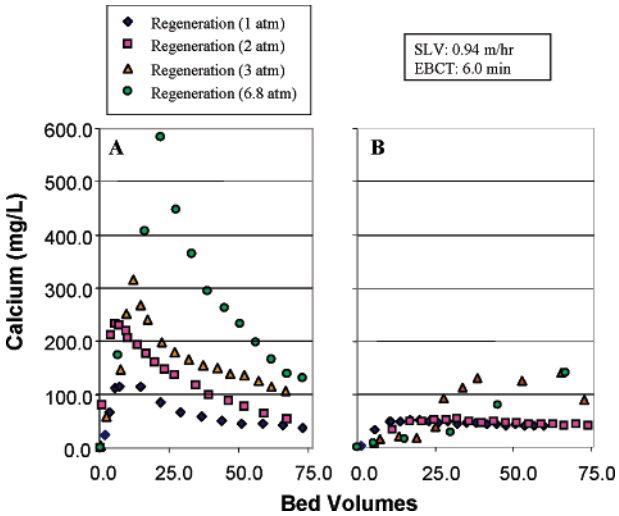

FIGURE 5. Effluent calcium concentration profiles for (A) IX-fibers and (B) resins during CO_2-sparged snowmelt regeneration at different carbon dioxide partial pressures.

proposed process. At near-neutral or under slightly alkaline conditions, calcium or other divalent ions are very selectively removed by IX-fibers in the presence of sodium ions. Conversely, calcium ions can be efficiently eluted by increasing the hydrogen ion concentration in the aqueous phase, i.e., reducing pH. To determine relative Ca^{2+}/H^+ affinity for IX-fibers, an equilibrium desorption test was carried out by sparging carbon dioxide in a batch reactor containing 10.0 g of calcium-loaded IX-fibers in 1.0 L of

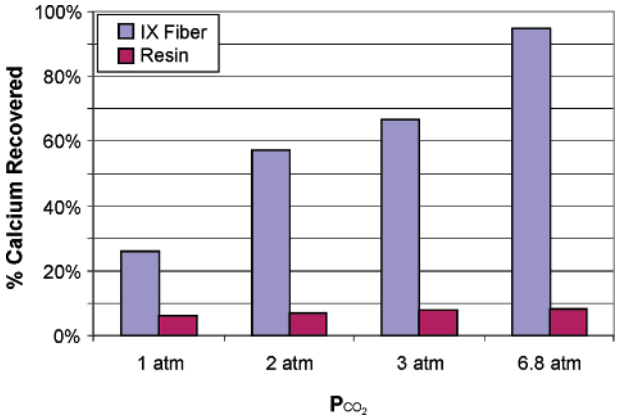

FIGURE 6. Percentage recoveries of calcium for both IX-fibers and resins during regeneration at different carbon dioxide partial pressures.

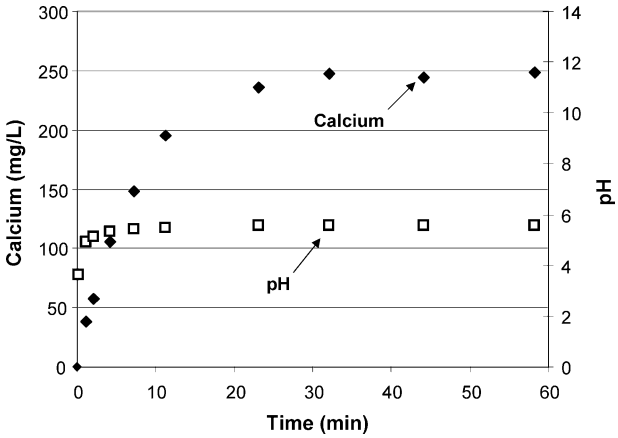

FIGURE 7. Equilibrium desorption test depicting both calcium and pH profiles during a batch regeneration at a carbon dioxide partial pressure of 1 atm.

distilled water. Figure 7 shows the results of the study. As already demonstrated, the desorption process was quite rapid, and nearly 26% of the calcium was eluted from the fibers at an equilibrium pH of 5.6. Equivalent concentrations of Ca^{2+} and H^+ at equilibrium in the fiber phase are as follows

$$[\overline{F-Ca}] = 3.8 \text{ mequiv/g}$$

$$[\overline{F-H}] = 1.1 \text{ mequiv/g}$$

The H^+/Ca^{2+} separation factor under the experimental conditions is

$$\alpha_{H/Ca} = \frac{[\overline{F-H}]}{[\overline{F-Ca}]}\frac{[Ca^{2+}]}{[H^+]} = 1675$$

A very high separation factor value in favor of hydrogen ion explains why a weak-acid gas, such as carbon dioxide, is an effective regenerant.

Evidence of Shrinking Beads. As described earlier, light microscopy tests were performed to monitor the relative shrinking of both weak-acid resin beads and IX-fibers as they are partially transformed from calcium to hydrogen forms. The results in the form of photographs are depicted in Figures 8A and 8B. Note that a spherical bead 490 μm in diameter shrank fairly rapidly to 402 μm under the experimental conditions in less than 10 min. The rate of shrinking, however,

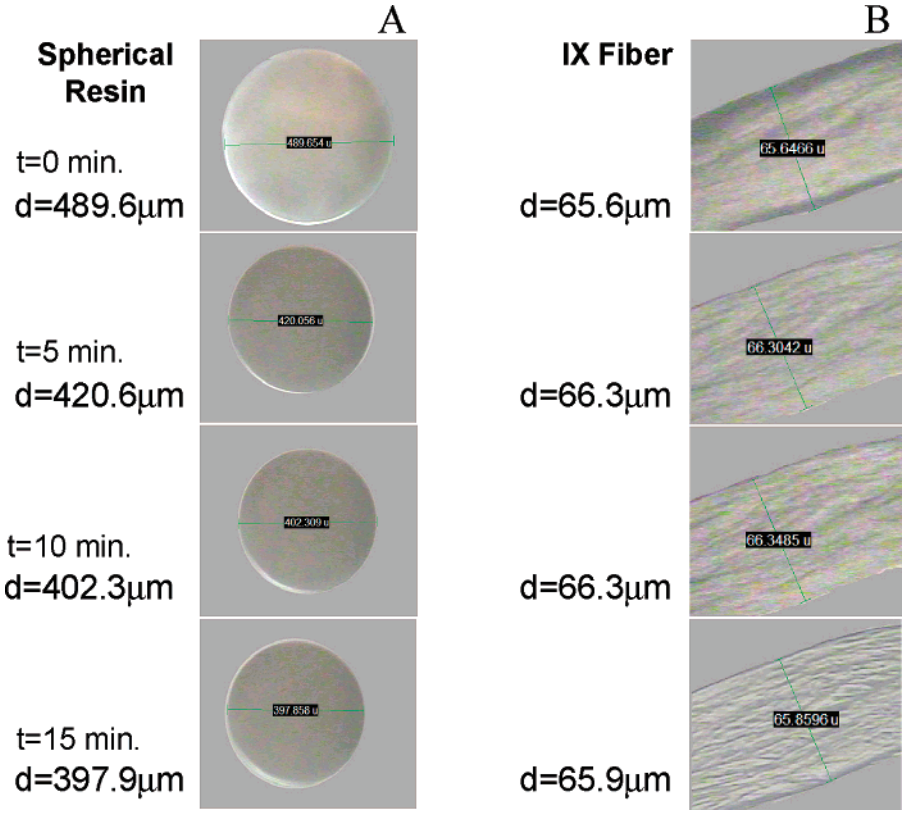

FIGURE 8. Light microscopy photographs detailing the physical changes of resin beads during their conversion from calcium to hydrogen form: (A) spherical resin beads; (B) IX-fibers.

gradually slowed, and no significant shrinking was observed after 10 min. For an enhanced sensitivity, the weak-acid IX-fiber chosen for the test under identical conditions had a relatively high cylindrical diameter (65 μm). Note that no significant change or trend in shrinking was observed during the course of the experiment (Figure 8B).

Discussion

Process Validation. Laboratory results in Figures 5 and 6 validate that snowmelt (or harvested rainwater) in conjunction with carbon dioxide can be an effective regenerant for elution of calcium or hardness from weak-acid ion-exchange fibers. A significant portion of the carbon dioxide consumed is sequestered in water for calcium desorption and converted into alkalinity in accordance with eq 6. Flue gases containing 16−18% carbon dioxide from oil- and gas-fired steam generators without any significant impurities can be good candidates for IX-fiber regeneration after necessary cooling. The fixed-bed columns containing IX-fibers can be reused for multiple cycles without requiring any aggressive chemicals such as mineral acids or high concentrations of sodium chloride. Snowmelt or harvested rainwater is an important ingredient for regeneration because it contains no alkalinity. Any natural water with low alkalinity is also suitable. In comparison, commercial weak-acid ion-exchange resins were not amenable to efficient regeneration with carbon-dioxide-sparged harvested snowmelt. The experimental observations that calcium removal capacities are independent of influent calcium concentrations (Figures 4A and 4B) validate that calcium uptake by fibers follows ion-exchange stoichiometry.

To assess the quantitative effect of the carbon dioxide partial pressure (P_{CO_2}) on the efficiency of regeneration, let us consider the overall equilibrium constant ($K_{overall}$) for reaction 6 at 298 K, i.e.,

$$\overline{(F-COO)_2Ca} + 2CO_2(g) + 2H_2O \Leftrightarrow \overline{2F-COOH} + Ca^{2+} + 2H_2CO_3 \quad (6)$$

$$K_{overall} = \frac{[\overline{F-COOH}]^2[Ca^{2+}][HCO_3^-]^2}{[\overline{(F-COO)_2Ca}]P_{CO_2}^{\ 2}} \quad (7)$$

Combining equilibrium constants for reactions 3−5

$$K_{overall} = (K_H)^2(K_{a1})^2K_{IX} \quad (8)$$

where K_H is the Henry's constant for CO_2 dissolution in water, K_{a1} is the first acid dissociation constant of carbonic acid, and K_{IX} is the equilibrium constant for the exchange between H^+ and Ca^{2+} with fibers. Considering ideality and rearranging eqs 7 and 8, we obtain

$$[Ca^{2+}][HCO_3^-]^2 = (K_H)^2(K_{a1})^2(K_{IX})\frac{[\overline{(F-COO)_2Ca}]}{[\overline{(F-COOH)}]^2}(P_{CO_2})^2 \quad (9)$$

From electroneutraility

$$2[Ca^{2+}] \approx [HCO_3^-] \quad (10)$$

For a given percentage of regeneration efficiency, calcium and hydrogen loading of the ion-exchange fibers are constant. After application of this condition, through the use of the

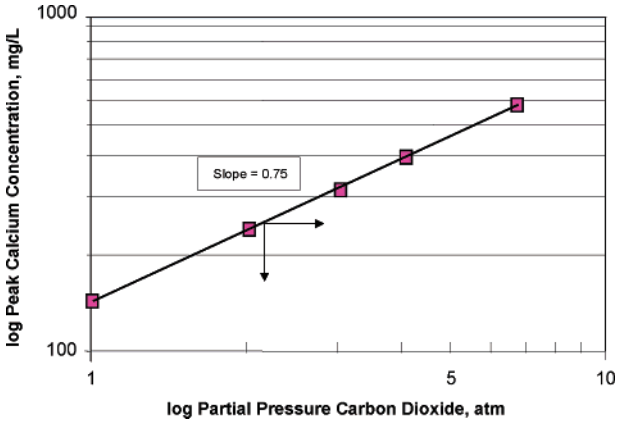

FIGURE 9. Maximum (peak) calcium concentrations during desorption versus applied carbon dioxide partial pressures for IX-fibers.

equality of eq 10, and assuming ideality in both phases, eq 9 degenerates into the following simplified form

$$[Ca^{2+}] = \text{constant } (P_{CO_2})^{2/3} \tag{11}$$

$$\log [Ca^{+}] = 0.67 \log P_{CO_2} + \log \text{constant} \tag{12}$$

Equations 11 and 12 demonstrate how calcium concentration during desorption is enhanced with an increase in the partial pressure of carbon dioxide. Maximum calcium concentrations from the desorption runs in Figure 5 for IX-fibers were recorded and plotted against applied carbon dioxide partial pressure in a log−log plot as shown in Figure 9. Note that despite some assumptions including ideality in both phases, the slope of the log Ca−log P_{CO_2} line is equal to 0.76 and close to the value predicted by eq 12.

Regeneration Efficiency. One of the striking findings of the investigation is that while the IX-fibers were amenable to efficient regeneration with CO_2-sparged snowmelt, commercial weak-acid ion-exchange resins (C-104) responded poorly to the same regeneration process. Spherical resin beads and IX-fibers are chemically similar; both have weak-acid carboxylate functional groups covalently attached to a polymer substrate. Their equilibrium properties are thus identical, and they exhibit high calcium removal capacity in the presence of competing sodium ions at near-neutral pH. However, due to the spherical geometry of the resin beads with sizes in the range of 400−1200 μm, the sorption kinetics are intraparticle diffusion controlled. The results of the interruption test in Figure 3 showed a significant drop in calcium concentration for resin beads following the restart of the column. As explained in several previous studies (*22*−*24*), this phenomenon represents predominant diffusional resistances within the resin beads. On the contrary, the drop in calcium concentration following interruption in the IX-fiber column was negligible under experimental conditions, suggesting liquid film diffusion as the predominant rate-limiting step. This observation is consistent with the results of kinetic studies carried out earlier with IX-fibers for other ions (*18*−*21*).

To develop a mechanistic understanding of the poor regenerability of calcium-loaded spherical resin beads with carbon dioxide, let us consider a single bead as a polyelectrolyte gel with carboxylate functional groups. The affinity sequence for weak-acid carboxylate functional groups stands as follows: $H^+ \gg Ca^{2+} > Na^+$. Uptake of H^+ during regeneration by a weak-acid carboxylate group is essentially an association reaction leading to a major decrease in its osmotic pressure, thus causing expulsion of water from the gel phase. A spherical ion-exchange resin bead, therefore, gradually shrinks with the progress of regeneration through the uptake of hydrogen ions that involves counter-transport of H^+ and Ca^{2+}. At the onset, hydrogen ions would initially displace the outermost (i.e., peripheral) calcium ions. Such an exchange would, however, dramatically decrease the water content of the regenerated portion, thus decreasing the overall intraparticle diffusivity near the outer periphery of the resin bead. The progress of the regeneration process increases the depth of the relatively impervious skin, thus further slowing down the counter-transport of H^+ and Ca^{2+}. Scientifically, this hypothesis is in agreement with the sequence of photographs taken during the light microscopy test (Figure 8A) and the premise of the ion-exchange kinetics accompanied by chemical reactions (*25*, *26*). Previous studies with weak-acid cation-exchange resins also provided optical confirmation of shrunk cores during acid regeneration (*27*). For carbon dioxide regeneration, hydrogen ion concentration in the bulk phase cannot be as high as it is normally with mineral acid regeneration. Thus, the concentration gradient across the shrunk core is too small to overcome the diffusional resistance. The poor regenerability of resin beads with carbon dioxide is thus attributed to enhanced diffusional resistance offered by the shrunk peripheral layers with very low water content.

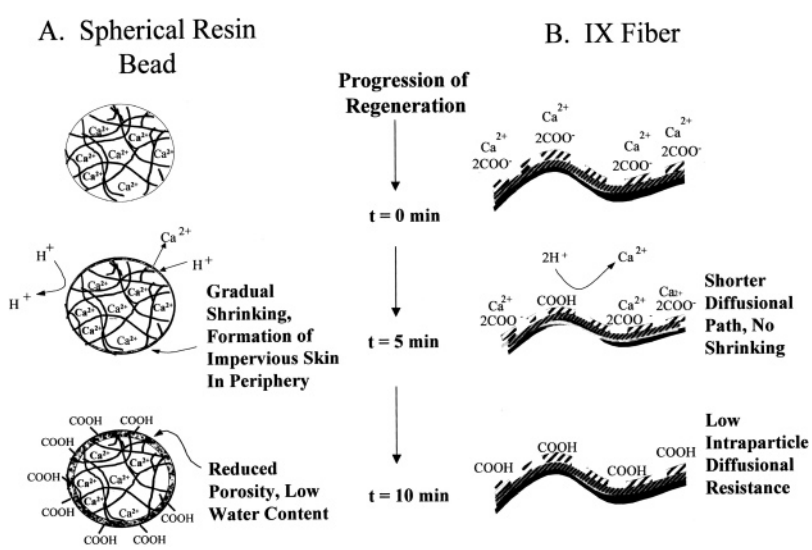

FIGURE 10. Schematic illustrating the difference in desorption mechanisms between (A) resin beads and (B) IX-fibers.

To the contrary, the ion-exchange sites for fibers reside primarily on the surface, and the phenomenon of intraparticle diffusion, as demonstrated earlier, is of lesser significance. Protonation of weak-acid functional groups has only marginal impact on diffusional resistance, and hence, the carbon dioxide regeneration is efficient for IX-fibers. Figures 10A and 10B illustrate the underlying difference in the regeneration mechanism of spherical resin beads and IX-fibers in sequential steps.

Acknowledgments

The authors are thankful to the United States Environmental Protection Agency for partial funding of the project through Technology for Sustainable Environment Grant No. RD-83143301. J. E. Greenleaf is thankful for the R. L. Johnson fellowship awarded to him during the summer of 2004.

Literature Cited

(1) AWWA Sludge Disposal Committee. Lime softening sludge treatment and disposal. *J. Am. Water Works Assoc.* **1981**, *11*, 600−609.
(2) AWWA Sludge Disposal Committee. Water treatment plant sludges—An update of the state of the art. *J. Am. Water Works Assoc.* **1978**, *9*, 498−503.
(3) Clifford, D.; Subramonian, S.; Sorg, T. J. Water treatment processes. III. Removing dissolved inorganic contaminants from water. *Environ. Sci. Technol.* **1986**, *20*, 1072−1080.
(4) Clifford, D. Ion exchange and inorganic sorption. In *Water Quality and Treatment: A Handbook of Community Water Supplies*, 5th ed.; AWWA, Letterman, R. D., Eds.; McGraw-Hill: New York, 1999; Chapter 9.
(5) Soldatov, V. S.; Shunkevich, I. S.; Elinson, I. S.; Johann, J.; Iraushek, H.; Chemically active textile materials as efficient means for water purification. *Desalination* **1999**, *124*, 181−192.
(6) Economy, J.; Dominguez, L.; Mangun, C. Polymeric ion-exchange fibers. *Ind. Eng. Chem. Res.* **2002**, *41*, 6436−6442.
(7) Perepelkin, K. E. Chemical fibers with specific properties for industrial application and personnel protection. *J. Ind. Text.* **2001**, *31*, 87−102.
(8) Jaskari, T.; Vuorio, M.; Kontturi, K. Ion-exchange fibers and drugs: An equilibrium study. *J. Controlled Release* **2001**, *70*, 219−229.
(9) Fiban Ion Exchange Fibers. Institute of Physical Organic Chemistry of the National Academy of Science of Belarus, Ecofil-Deco, 2002. http://ifoch.bas-net.by/res_eng.htm; http://ifoch-.bas-net.by/K4_eng1.htm.
(10) Dominguez, L.; Benak, K. R.; Economy, J. Design of high efficiency polymeric cation exchange fibers. *Polym. Adv. Technol.* **2001**, *12*, 197−205.
(11) Liquan, C.; Zhang, W.; Zhong, Z. Study of ion chromatography with ion-exchange fibers and the stationary phase. *J. Chromatogr., A* **1996**, *740*, 195−199.
(12) Jyo, A.; Kugara, J.; Trobradovic, H.; Yamabe, K.; Sugo, T.; Tamada, M.; Kume, T. Fibrous iminodiacetic acid chelating cation exchangers with a rapid adsorption rate. *Ind. Eng. Chem. Res.* **2004**, *437*, 1599−1607.
(13) Hoell, W. H.; Feuerstein, W. Partial demineralization of water by ion exchange using carbon dioxide as a regenerant. Part III. Field tests for drinking water treatment. *React. Polym.* **1986**, *4*, 147−153.
(14) Hoell, W. H. CARIX Process—A novel approach to desalination by ion exchange. In *Ion Exchange Technology Advances in Pollution Control*; SenGupta, A. K., Ed.; Technomic: Lancaster, PA, 1995; pp 271−313.
(15) SenGupta, A. K.; Lim, L. Modeling chromate ion-exchange processes. *AIChE J.* **1988**, *34*, 2019.
(16) Zhao, D.; SenGupta, A. K. Ultimate removal of phosphate using a new class of an ion exchanger. *Water Res.* **1998**, *32*, 1613−1625.
(17) Cumbal, L.; SenGupta, A. K. Arsenic removal using polymer-supported hydrated iron(III) oxide nanoparticles: Role of donnan membrane effect. *Environ. Sci. Technol.* **2005**, *39*, 6508−6515.
(18) Petruzzelli, D.; Kalinitchev, A.; Soldatov, V. S. Chloride/sulfate ion exchange kinetics on fibrous resins. *Ind. Eng. Chem. Res.* **1995**, *34*, 2618−2624.
(19) Lin, W.; Hsieh, Y. L. Kinetics of metal ion absorption on ion-exchange and chelating fibers. *Ind. Eng. Chem. Res.* **1996**, *35*, 5. 3817−3821.
(20) Vuorio, M.; Manzanares, J. A.; Murtomaki, L.; Hirvonen, J.; Kankkunen, T.; Kontturi, K. Ion exchange fibers and drugs a transient study. *J. Controlled Release* **2003**, *91*, 439−448.
(21) Chen, L.; Yang, G.; Zhang, L. A study on the exchange kinetics of ion exchange fibers. *React. Funct. Polym.* **1996**, *29*, 139−144.
(22) Li, P.; SenGupta, A. K. Intraparticle diffusion during selective ion exchange with a macroporous ion exchanger. *React. Polym.* **2000**, *44*, 273−287.
(23) DeMarco, M. J.; SenGupta, A. K.; Greenleaf, J. Arsenic removal using a polymeric/inorganic hybrid sorbent. *Water Res.* **2003**, *37*, 164−176.
(24) Li, P.; SenGupta, A. K. Intraparticle diffusion during sorption of trace contaminants: effect of gel verus macroporous morphology. *Environ. Sci. Technol.* **2000**, *34*, 5193−2000.
(25) Helfferich, F. Ion exchange kinetics: V. Ion exchange accompanied by chemical reactions. *J. Phys. Chem.* **1965**, *69*, 1178−1187.
(26) Hoell, W. H.; Sontheimer, H. Kinetics of the protonation of weak-acid ion-exchange resins. *Chem. Eng. Sci.* **1977**, *32*, 755−762.
(27) Hoell, W. Optical verification of ion exchange mechanisms in weak electrolyte resins. *React. Polym.* **1981**, *2*, 93−101.

Received for review August 26, 2005. Revised manuscript received October 17, 2005. Accepted October 18, 2005.

ES051702X